

INVESTIGATION OF HOT CORROSION BEHAVIOUR OF PLASMA SPRAYED CNTS-ALUMINA COATED ASME-SA213-T22(T22)BOILER TUBE STEEL IN ACTUAL BOILER ENVIRONMENT

Rakesh Goyal¹, Buta Singh Sidhu² & VikasChawla³

Abstract- In this work, carbon nanotubes reinforced Al₂O₃ coated T22 boiler tube steel was investigated for hot corrosion behaviour at 900 °C temperature in actual boiler environment. The coatings were deposited using plasma spray technique and Ni-Cr was used as bond coat before applying CNTs-Al₂O₃ coatings. The hot corrosion studies were conducted on uncoated as well as plasma spray coated specimens in actual boiler of thermal power plant. X-ray diffraction (XRD), scanning electron microscopy, energy-dispersive x-ray analysis (SEM, EDAX) techniques were used to analyse the corrosion products. The CNTs reinforced alumina coatings enhance resistance to corrosion significantly.

Keywords: hot corrosion, Thermal spray, Carbon nanotubes, boiler steel, XRD,SEM, EDAX

1. INTRODUCTION

The hot corrosion is severe phenomenon which affects the metals and alloys at high temperature, when they are heated in air[1, 2]. The rate of corrosion increases with further increase in temperature[3-5]. The steel alloys tubes are used to manufacture boilers which are used in high temperature environment in thermal power plants and industrial waste incinerators[6, 7]. These steel tubes are often subjected to high temperature stresses due to variation in temperature[8-10]. The steel tubes are unable to resist high temperature corrosion in the boilers. Therefore, to protect the surface of boiler tubes, protective coatings are used to counter the corrosion. The thermal spraying techniques are used to apply these coatings on the boiler tubes. Plasma spraying is one of the important thermal spraying technique to apply coatings on boiler tube steels [8, 11-13]. A combination of metals and ceramics can be deposited on the steels using plasma spraying technique [14]. Plasma sprayed coatings of various ceramic materials such as Alumina (Al₂O₃), calcia (Ca)-stabilized zirconia (ZrO₂) and other refractory materials have been produced for different high temperature applications [12, 14-16]. Alumina is an incredibly imperative ceramic material which has numerous innovative applications. It has high hardness, chemical inertness and high liquefying point. It has ability to retain more than 90% of its strength even at 1100 °C [17]. It is reported that the alumina coatings have higher corrosion resistance than that of cermet and metallic coatings [18]. One of limitations of thermal sprayed coatings is that these coatings consist of cracks or voids at splat boundaries, and these coatings are attacked through these voids [19-22]. Therefore, there is still scope to improve the corrosion resistance of these coatings [23]. CNTs were invented in 1991, and are having exceptionally high mechanical and electrical properties as compared to that of the high grade carbon steels [24-27]. These properties of CNTs make them a potential reinforcement material in composites [28-30]. A few researchers have developed CNTs based composite coatings and found that CNTs were able to enhanced the corrosion resistance of conventional coatings [31, 32]. Few researchers have studied the tribological behaviour of CNTs-Al₂O₃ composite coatings [33-36]. But no studies on CNTs-Al₂O₃ composite coatings for high temperature corrosion behaviour of boiler tube steel in actual boiler environment are available. Therefore, there is scope of investigating hot oxidation behaviour of CNTs-Al₂O₃ composite coatings on boiler steel in actual boiler environment.

In the present study high temperature corrosion behaviour of plasma sprayed alumina and 1.5 wt.%, 2 wt.%, and 4 wt.% CNTs-Al₂O₃ composite coatings deposited on T22 boiler steel is investigated in actual boiler environment. The techniques used are metallography, SEM, EDAX and XRD to study the corrosion products.

2. EXPERIMENTAL PROCEDURE

2.1 Substrate Material and Coating Material

T22 boiler tube steel was selected for this study. Actual and nominal composition of T22 steel is given in Table 1. The sample sizes of 20 mm × 15 mm × 5 mm size were prepared by cutting T22 boiler tube steel.

¹ Corresponding Author, Mechanical Engineering Department, I.K.G. PTU, Kapurthala, 144603, Mechanical Engineering Department, Chitkara University, Rajpura, 144401 India

² Mechanical Engineering Department, M.R.S. PTU, Bathinda, 151001, India

³ Mechanical Engineering Department, I.K.G. PTU, Kapurthala, 144603, India

Table 1 Chemical composition (wt.%) of substrate steel.

Boiler steel	ASME code	Composition	C	Mn	Si	S	P	Cr	Mo	V	Ni	Fe
T22	SA213-T22	Nominal	0.15	0.3-0.6	0.5-1	0.03	0.03	1.9-2.6	0.87-1.13	-	-	Bal.
		Actual	0.0863	0.5337	0.7164	0.008	0.0115	2.630	0.29	0.0243	0.106	Bal.

Different coating powders were prepared by mixing Al₂O₃ powder with 1.5 wt.%, 2 wt.%, and 4 wt.% CNTs in a ball mill. Table 2 shows the chemical composition and particle sizes of different coating powders.

Table 2 Composition of the feed stock powders

Feedstock powder	Chemical composition, wt.%	Particle size	Shape
Al ₂ O ₃	Al ₂ O ₃	40µm±10µm	Angular
Al ₂ O ₃ -1.5% CNT	98.5% Al ₂ O ₃ -1.5% CNT	40µm±10µm	Angular
Al ₂ O ₃ -2 % CNT	98% Al ₂ O ₃ -2 % CNT	40µm±10µm	Angular
Al ₂ O ₃ -4% CNT	96% Al ₂ O ₃ -4% CNT	40µm±10µm	Angular

The coatings have been deposited on the boiler tube steel substrates by using Air Plasma spray system. First, Ni-Cr powder was sprayed as bond coat on the substrates.

2.2 High temperature corrosion experiments

The experiments were performed in superheater of the boiler of Guru Nanak Dev Thermal Plant, Bathinda, Punjab, India. The specimens were hung at 31 m height from the boiler base with the help of a stainless steel wire through the soot blower dummy holes. The average temperature in the boiler was 900°C with a variation of ±15°C. The specimens were exposed to the actual environment for 10 cycles. Each cycle was consisting of 100 hrs. heating and 1 hr. cooling. Because of the ash deposition on the specimens, the weight change data could not be used directly for predicting degradation behaviour. Therefore, degradation was assessed using cumulative weight gain data, metal thickness loss and depth of corrosion attack. XRD, FE-SEM, EDS and X-ray mapping techniques were used to analyse the corrosion products.

3. RESULTS

3.1 Visual Examination

The macrographs of the bare and Al₂O₃-CNT coated T22 steel samples after 1000 hrs. exposure (each cycle of 100 hrs. heating and 1 hr. cooling), in the platen superheater of coal fired boiler are shown in Fig. 1. Bare T22 steel suffered corrosion attack due to the formation of porous oxide scale as shown in Fig. 1 (a).

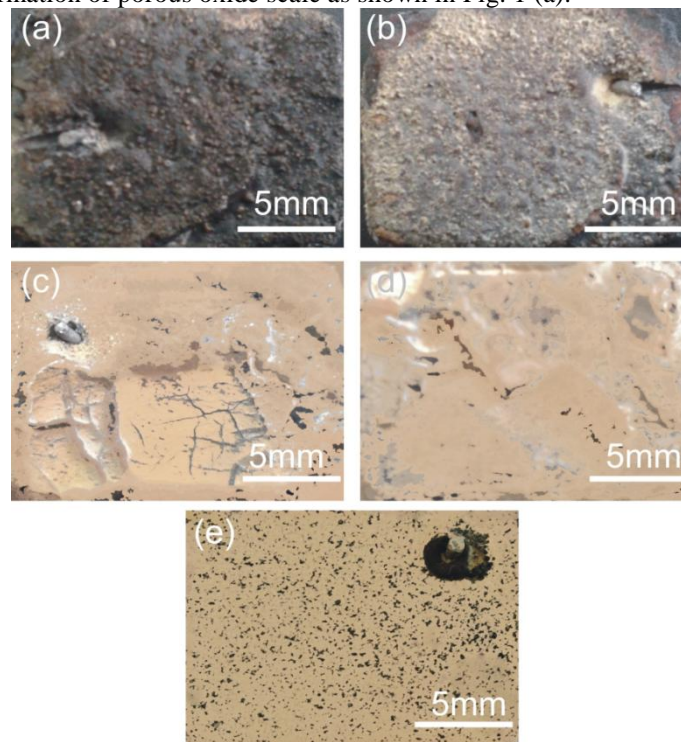


Fig.1 Macrographs of the T22 steel samples: (a) Uncoated T22 boiler steel, (b) Al₂O₃ coating, (c) Al₂O₃-1.5% CNT coating, (d) Al₂O₃-2% CNT coating, (e) Al₂O₃-4% CNT coating

Corresponding macrographs of Conventional Al_2O_3 coated, Al_2O_3 -1.5% CNT coated, Al_2O_3 -2% CNT coated and Al_2O_3 -4% CNT coated T22 steel are shown in Fig. 1 (b-e). The physical conditions of the exposed specimens such as changes in the colour, spallation, cracks in the surface, etc., if any, can be observed from the macrographs.

3.2 Weight Change Data and Thickness Monitoring

Figure 2 shows the cumulative weight gain/unit area (mg/cm^2) for bare and Al_2O_3 -CNTs coated T22 steel up to the end of the cyclic study. The net weight gain of the specimens in the given environment represents the resulting effect of the weight gain owing to the formation of the oxide scales. The overall weight gain by the bare steel has been found to be $104.6 \text{ mg}/\text{cm}^2$. Bare T22 steel showed higher weight gain than coated specimen due to the formation of thick oxide scale. The weight gain of Conventional Al_2O_3 coated T22 steel has been found to be $66.82 \text{ mg}/\text{cm}^2$. The overall weight gain of Al_2O_3 -1.5% CNT coated, Al_2O_3 -2% CNT coated and Al_2O_3 -4% CNT coated T22 steel was found to be 34.11, 16.47 and $10.16 \text{ mg}/\text{cm}^2$ respectively.

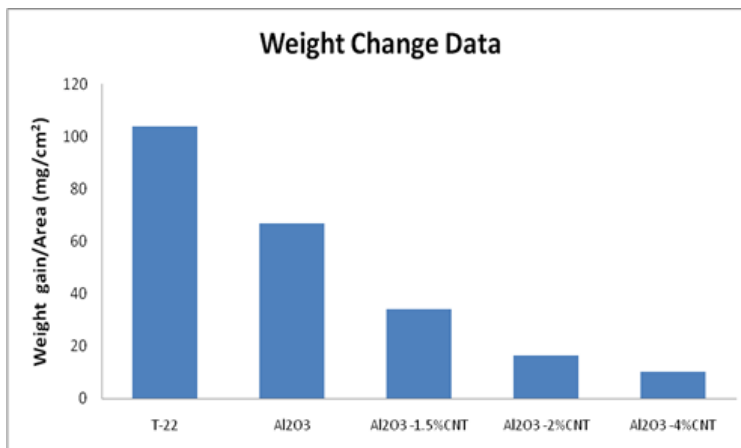


Fig. 2 Bar chart showing cumulative weight gain per unit area for (a) Uncoated T22, (b) Al_2O_3 coating, (c) Al_2O_3 -1.5% CNT coating, (d) Al_2O_3 -2% CNT coating, (e) Al_2O_3 -4% CNT coating

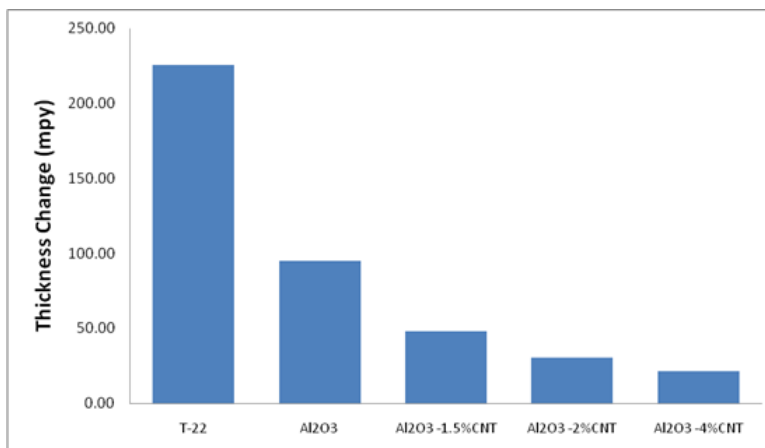


Fig. 3 Bar chart indicating the thickness change in mils per year (mpy) by the (a) Uncoated T22, (b) Conventional Al_2O_3 coating, (c) Al_2O_3 -1.5% CNT coating, (d) Al_2O_3 -2% CNT coating, (e) Al_2O_3 -4% CNT coating

It indicates that with the increase in CNTs content in the conventional Al_2O_3 coating, the overall weight gain of the coated steel decreases. Al_2O_3 -4% CNT coated T22 steel showed minimum overall weight gain amongst all types of coatings. The thickness of metal lost by the bare steel is 1.012 mm as indicated in Fig. 3. The corrosion rates have been calculated based upon this thickness data in term of mils per year (mpy). Corrosion rate indicated by T22 steel is 225.28 mpy. Based upon the thickness loss data as presented in Fig. 3, the corrosion rates indicated by these coatings are 95.06, 48.08, 30.27 and 21.37 mpy for conventional Al_2O_3 , Al_2O_3 -1.5% CNT coated, Al_2O_3 -2% CNT coated and Al_2O_3 -4% CNT respectively.

3.3 X-ray Diffraction Analysis

X-ray diffraction analysis for the bare and coated T22 steel with conventional Al_2O_3 , Al_2O_3 with 1.5 wt.%, 2 wt.%, and 4 wt.% CNTs coatings after exposure to a platen superheater of the coal fired boiler for 1000 hrs. at 900°C is shown in Fig. 4 to 8. The analysis for the bare T22 steel (Fig. 4) indicated the formation of mainly Fe_2O_3 in the oxide scale.

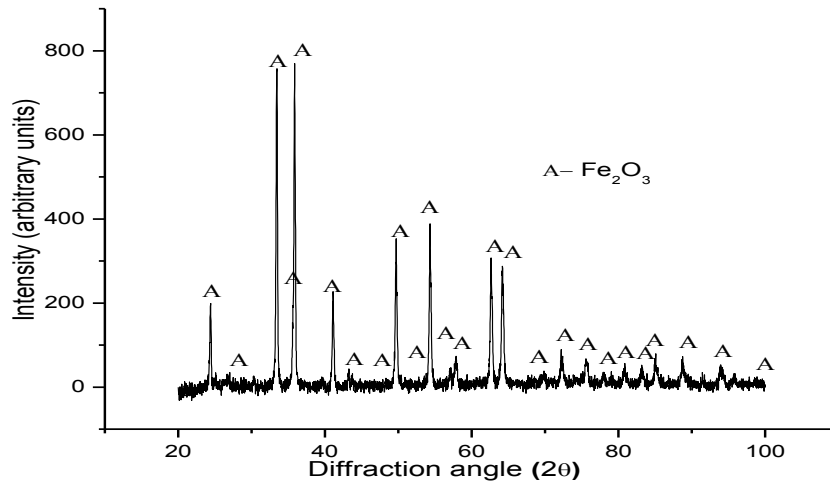


Fig. 4 XRD pattern for the uncoated T22 boiler steel

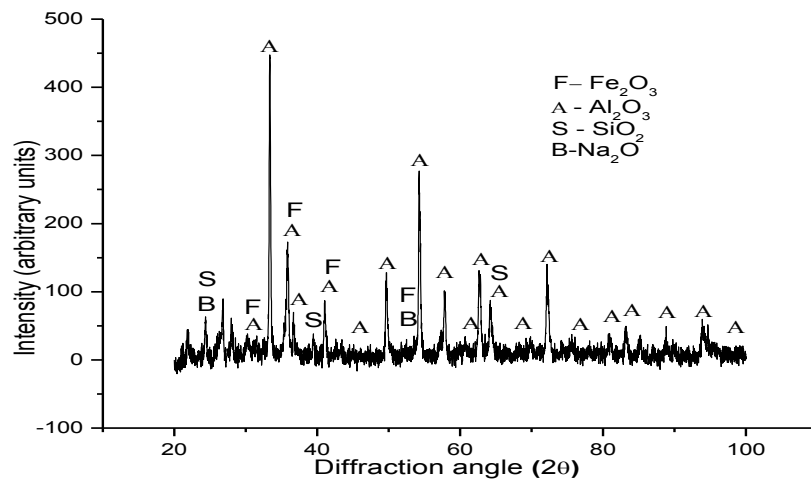


Fig. 5 XRD pattern for the plasma-sprayed Al₂O₃ coated T22 boiler steel

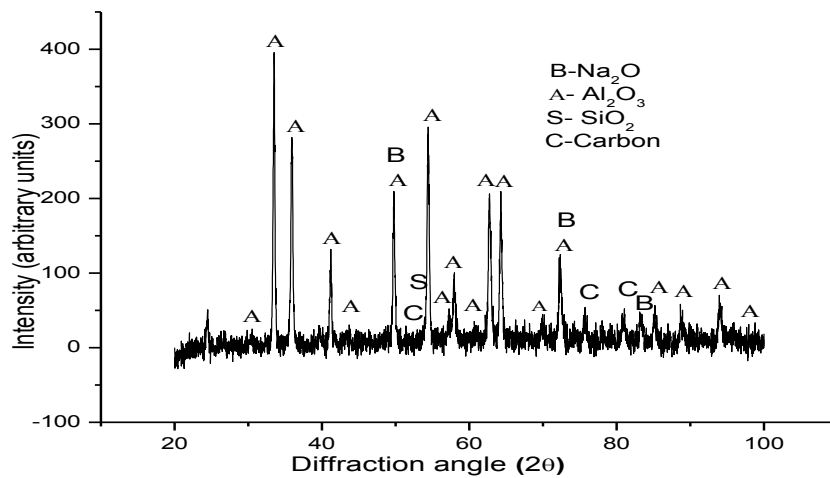


Fig. 6 XRD pattern for the plasma-sprayed Al₂O₃-1.5% CNT coated T22 boiler steel

Al_2O_3 was the main phase in the Al_2O_3 coated T22 steel after oxidation cycles (Fig. 5) along with Fe_2O_3 phase. In case of Al_2O_3 -1.5 wt.% CNTs coated T22 steel (Fig. 6) Al_2O_3 and C were observed as the main XRD phases. In the case of Al_2O_3 -2 wt.% CNTs coated T11 steel (Fig. 7), Al_2O_3 were the main XRD phases. In the case of Al_2O_3 -4 wt.% CNTs coated T22 steel (Fig. 8), Al_2O_3 and C were observed as the main XRD phases.

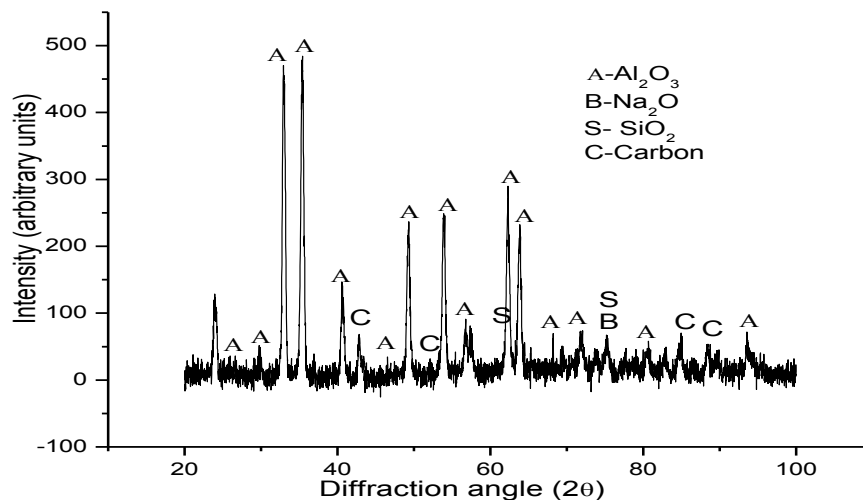


Fig. 7 XRD pattern for the plasma-sprayed Al_2O_3 -2% CNT coated T22 boiler steel

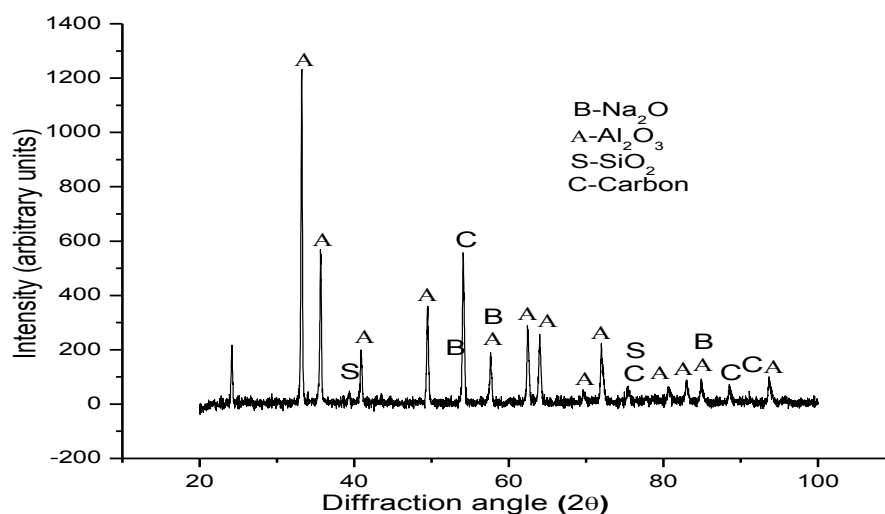


Fig. 8 XRD pattern for the plasma-sprayed Al_2O_3 -4% CNT coated T22 boiler steel

3.4 FE-SEM/EDS Analysis

The FE-SEM/EDS analysis of the bare and coated T22 boiler after exposure to a platen superheater of the coal-fired boiler for 1000 hrs. at 900°C is shown in Fig. 9. Oxide scale of bare T22 steel shown in Fig. 9 (a), indicates the appearance of irregular flakes with random orientation. The scale appears to be porous. The excessive corrosion could be seen on the surface of the specimen. The EDS analysis clearly indicates that the oxide scale composed mainly of iron and oxygen with the possible formation of Fe_2O_3 . The micrograph for the conventional Al_2O_3 coating is represented in Fig. 9 (b), which indicates small size nodular structure. As revealed by the EDS analysis, the composition is having mainly Fe, O and Al elements. The scale appears to be porous, and voids can be clearly seen. The micrograph of Al_2O_3 -1.5% CNT coated T22 steel is shown in Fig. 9 (c). It indicates the amount of O is more than the amount of Al in the composition and there is minor percentage of C in the scale. The EDS analysis for the scale of Al_2O_3 -2% CNT coated T22 steel shown in Fig. 9 (d), indicates the presence of Al, O, and C. The FE-SEM micrograph of Al_2O_3 -4% CNT coated T22 steel shown in Fig. 9 (e). It is clearly seen the presence of O, Al, and C in the scale.

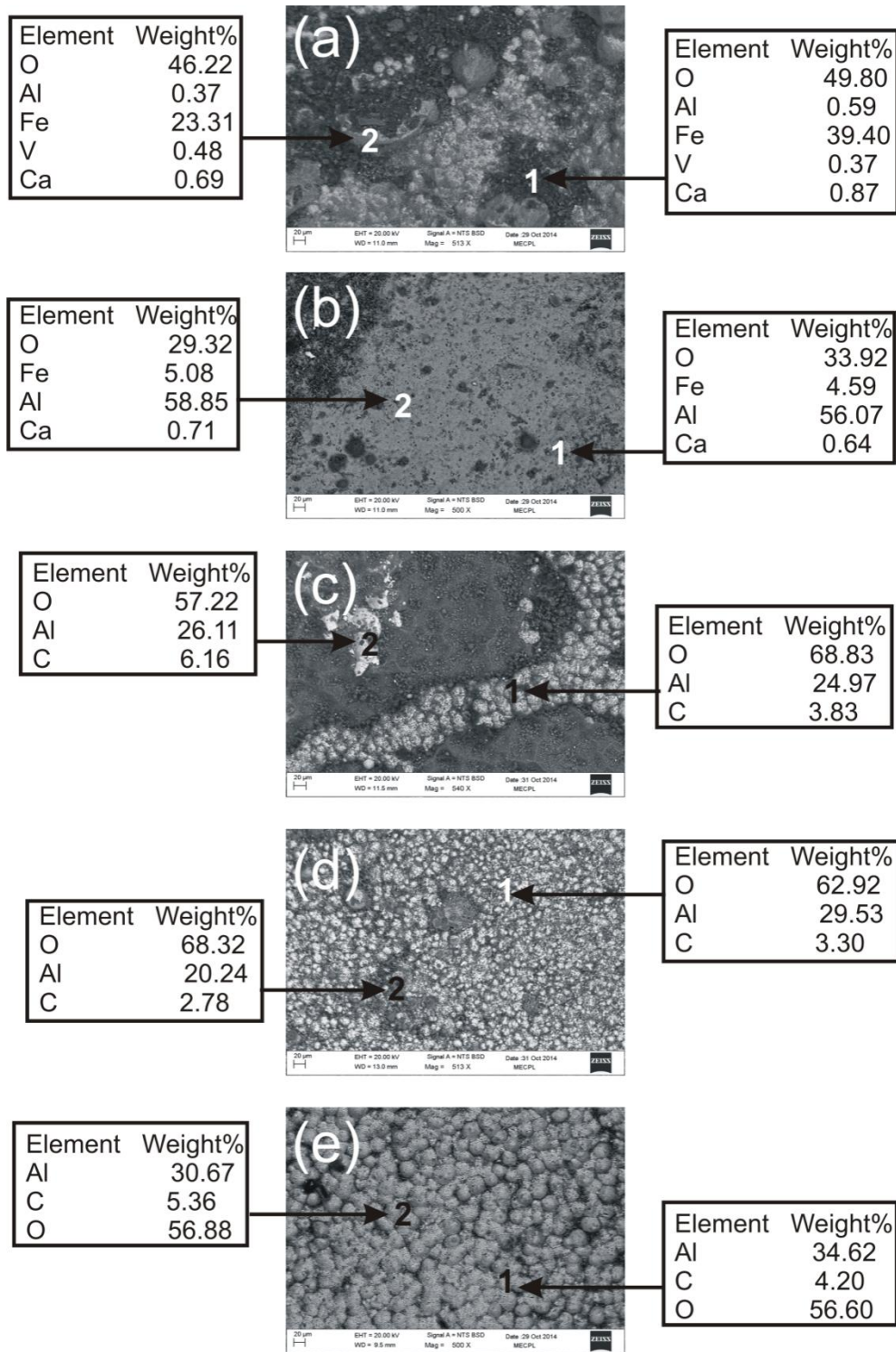


Fig. 9 FE-SEM/EDS analysis for the uncoated and coated T22 boiler steel: (a) Uncoated T11, (b) Al₂O₃ coating, (c) Al₂O₃-1.5% CNT coating, (d) Al₂O₃-2% CNT coating, (e) Al₂O₃-4% CNT coating

3.5 Cross-sectional analysis of the scale

The cross-sectional FE-SEM, EDS for the bare and coated T22 exposed is presented in Fig.10 to Fig.14. SEM micrograph of the bare T22 steel in Fig.10 shows cracks and dark spots in the scale with the significant amount of corrosion. Scale mainly consists of Fe, and O (point 2 to 6) clearly indicates the presence of oxides of iron. Fig. 11 shows SEM micrograph, and variation in elemental composition across the cross-section of the plasma-sprayed Al₂O₃ coated T22 boiler steel after exposure. The scale consists of Al, Fe, and O mainly clearly indicating the presence of oxides of Aluminium and Ferrous. The voids and black spots can be seen in the coating scale. Oxide scale morphology and EDS

analysis for the cross-section of Al_2O_3 -1.5% CNT coating is shown in Fig. 12. The scale appears to be adherent to the substrate. Inclusions can be seen at the interface. In scale, the C can be seen in major proportion (point 4 to 7), indicates the presence of CNTs in the coating matrix. SEM micrograph and variation in elemental composition along the cross-section of the plasma-sprayed Al_2O_3 -2% CNT coated T22 boiler steel after exposure is shown in Fig. 13.

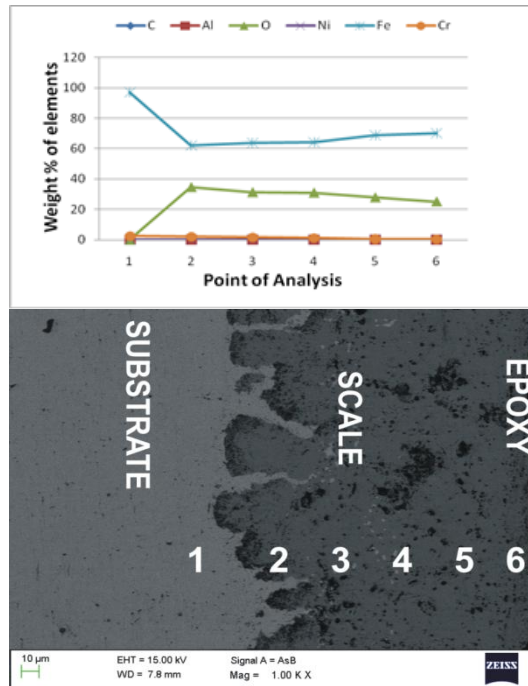


Fig. 10 SEM micrograph and variation in elemental composition across the cross-section of the T22 steel

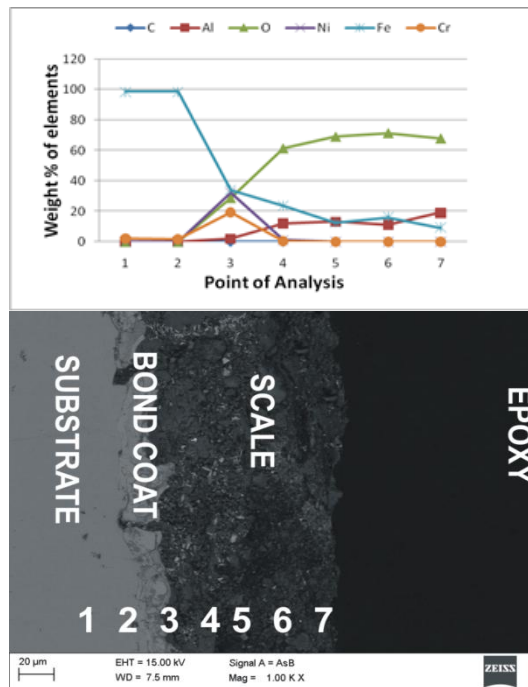


Fig.11 SEM micrograph and variation in elemental composition across the cross-section of the plasma-sprayed Al_2O_3 coated T22 steel

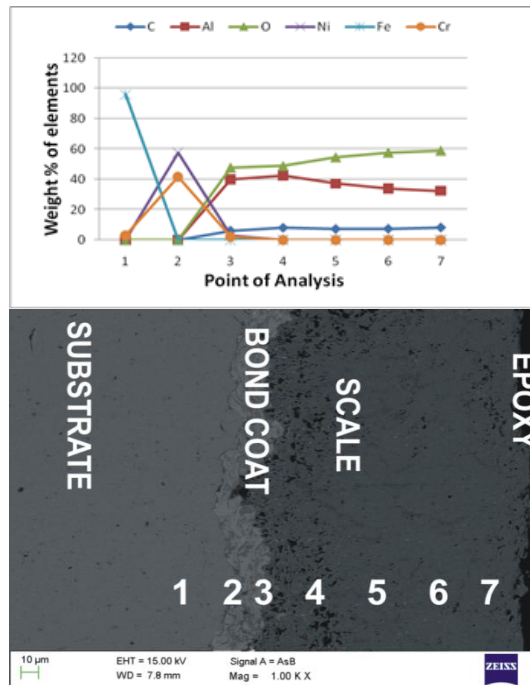


Fig.12 SEM micrograph and variation in elemental composition across the cross-section of the plasma-sprayed Al₂O₃-1.5% CNT coated T22 steel

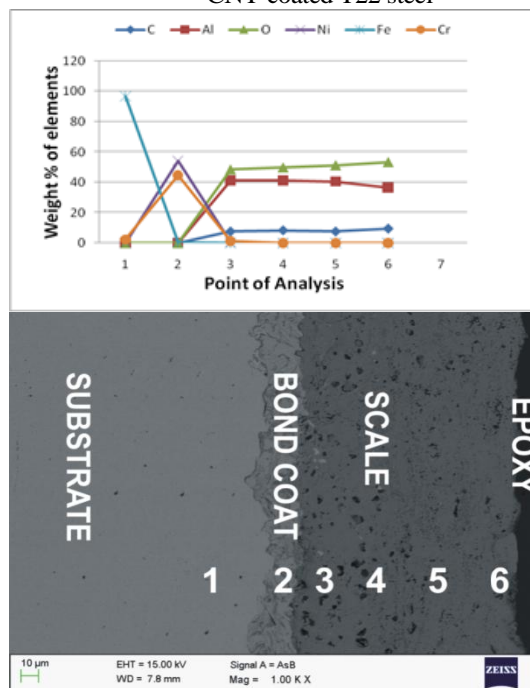


Fig.13 SEM micrograph and variation in elemental composition across the cross-section of the plasma-sprayed Al₂O₃-2% CNT coated T22 steel

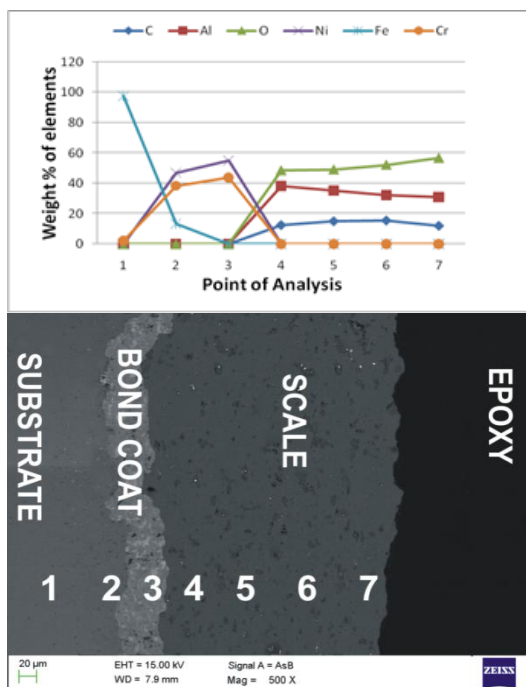


Fig. 14 SEM micrograph and variation in elemental composition across the cross-section of the plasma-sprayed Al_2O_3 -4% CNT coated T22 steel

3.6 X-ray Mapping Analysis

Composition image and elemental mappings for the cross-section of bare and coated T22 boiler steel are presented in Fig. 15 to Fig. 19. The SEM of the scale of bare T22 steel is shown in Fig. 15, shows the significant corrosion attack along the scale substrate interface and resulted in the formation of oxide scale. The oxygen has been penetrated into the substrate. The scale is mainly composed of an oxide of iron. Composition image and X-ray mappings along the cross-section of the Al_2O_3 coated T22 boiler steel after exposure is presented in Fig. 16. Fe is mainly presented in the substrate. The coating scale mainly consists of Al, Fe, and O clearly indicating the presence of aluminium oxide and Ferrous oxide in the scale. Composition image (SEI) and elemental mappings for the cross-section of Al_2O_3 -1.5% CNT coated T22 boiler steel is presented in Fig. 17. Scale mainly consists of Al and O along with C. Composition image (SEI), and elemental mappings for the cross-section of Al_2O_3 -2% CNT coated T22 boiler steel is presented in Fig. 18. Scale mainly consists of Al, C and O. Presence of C in the coating scale reveals the presence of CNTs in the alumina matrix. Fig. 19 shows the composition image (SEI) and elemental mappings for the cross-section of Al_2O_3 -4% CNT coated T22 boiler steel. The interface of coating and substrate is having the presence of Ni and Cr indicates the presence of bond coat adjoining the substrate.

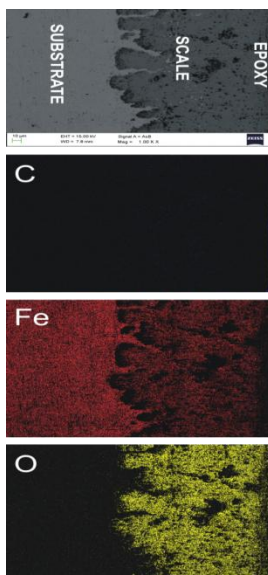


Fig. 15 Composition image and X-ray mappings across the cross-section of the T22 boiler steel

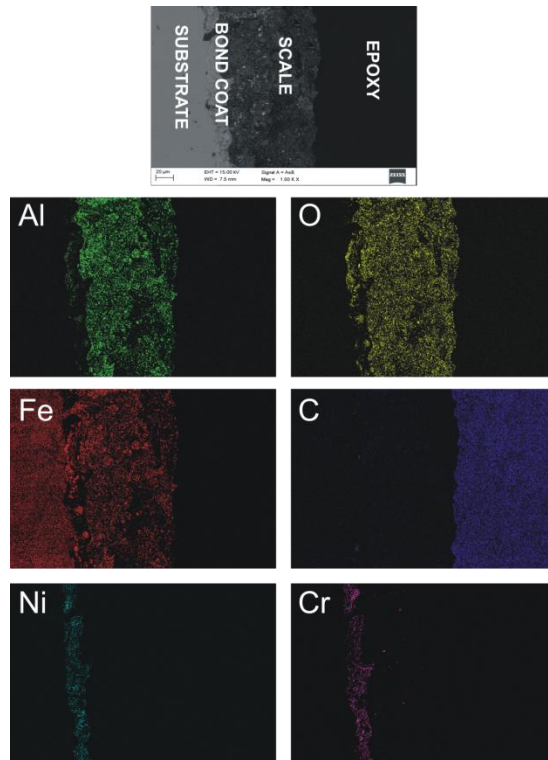


Fig. 16 Composition image and X-ray mappings across the cross-section of the plasma-sprayed Al₂O₃ coated T22 boiler steel

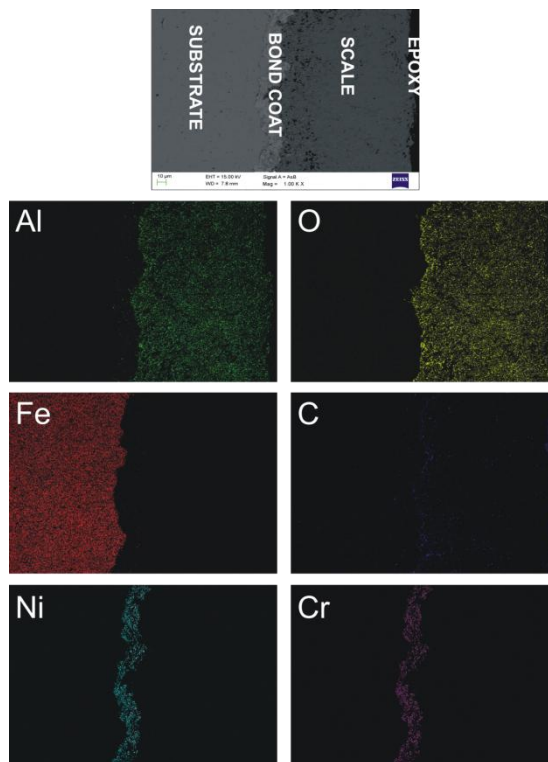


Fig. 17 Composition image and X-ray mappings across the cross-section of the plasma-sprayed Al₂O₃-1.5% CNT coated T22 boiler steel

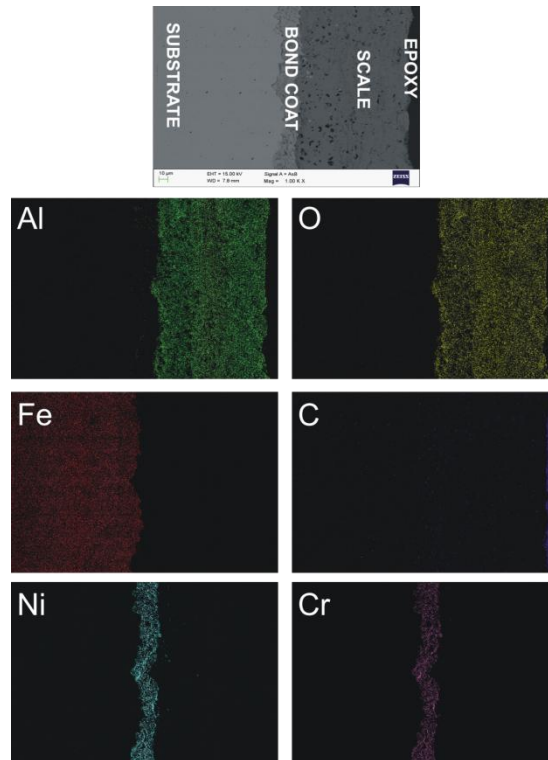


Fig. 18 Composition image and X-ray mappings across the cross-section of the plasma-sprayed Al_2O_3 -2% CNT coated T22 boiler steel

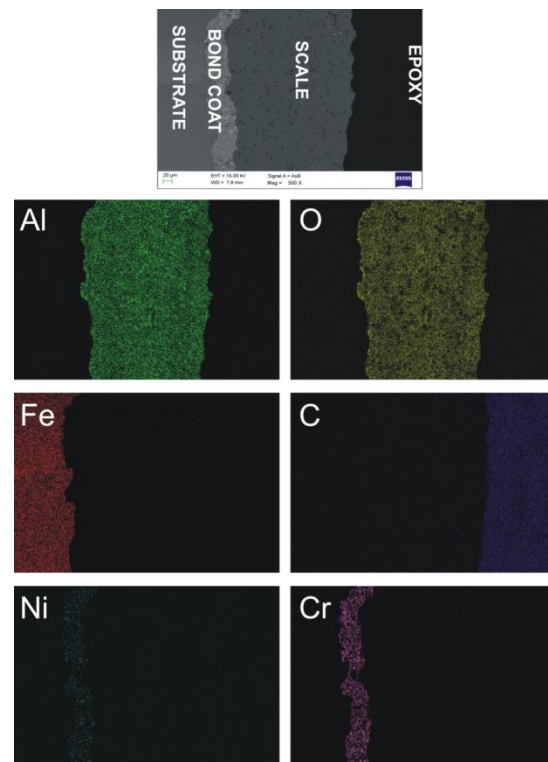


Fig. 19 Composition image and X-ray mappings across the cross-section of the plasma-sprayed Al_2O_3 -4% CNT coated T22 boiler steel

4. DISCUSSION

The bare T22 steel indicated severe corrosion after exposure to a platen superheater of the coal-fired boiler for 1000 hrs. at 900°C . The graphs of commutative weight gain vs. time have been shown in Fig. 2. The weight gain value for uncoated T22 specimen has been found to be 104.06 mg/cm^2 . The significant increase in weight during the study may be due to rapid oxygen pick up by the diffusion of oxygen and this is identical to the results reported in the literature [5, 37-41]. From the

XRD analysis of specimens, it is found that Fe_2O_3 phase was formed in bare steel specimen. The formation of Fe_2O_3 has been reported in the literature by Chawla [42], Somasundaram, et al. [43], Zhu, et al. [44] and Ramesh, et al. [40]. The XRD analysis has been further supported by FE-SEM/EDS analysis of these bare steels. The oxide scale of these steels indicated irregular flakes which are randomly oriented. The EDS analysis of given boiler steels clearly indicates that the oxide scale composed mainly of iron and oxygen with the formation of Fe_2O_3 . The cross-section analysis of all steels indicated loosely bounded scale with the significant amount of oxidation. Singh and Singh [45], Bala, et al. [46], Jegadeeswaran, et al. [37] and Gond, et al. [47] reported that the higher rate of oxidation might be due to loosely bounded scale. The scale further led to cracking due to different coefficients of thermal expansion of oxides in the scale [38, 48-50]. For Al_2O_3 -CNT coated T22 steel, the cumulative weight gain for Al_2O_3 -1.5% CNT coating is 34.11 mg/cm^2 , for Al_2O_3 -2% CNT coating is 16.47 mg/cm^2 , and for Al_2O_3 -4% CNT coating is 10.16 mg/cm^2 . The Al_2O_3 -1.5% CNT coating was successful to reduce the overall weight gain rate by 67.22% of that of bare T22 steel. Whereas, The Al_2O_3 -2% CNT coating was successful to reduce the overall weight gain rate by 84.18% of that of bare T22 steel and the Al_2O_3 -4% CNT coating was successful to reduce the overall weight gain rate by 90.24% of that of bare T22 steel. XRD graphs indicated the formation of Al_2O_3 phase in the coating during hot corrosion. SiO_2 and Na_2O have been formed after the exposure of specimens. The formation of these compounds has also been described by Ahmad, et al. [51]. The presence of these compounds may have acted as a barrier to the further weight gain due to oxidation. The presence of carbon has also been indicated in XRD analysis. The formation of these compounds has been further validated by X-ray mapping and elemental analysis. The presence of C indicated the presence of CNTs in the oxide scale. The cluster of CNTs was not observed, which indicated the uniform dispersion of CNTs in the coating matrix, which was able to reduce cumulative weight gain during the study.

5. CONCLUSIONS

In this research work, the high temperature oxidation behaviour of bare T22, conventional Al_2O_3 coated T22, 1.5 wt.%, 2 wt.%, and 4 wt.% CNTs- Al_2O_3 coated T22 was investigated at 900 °C in actual boiler environment. The following conclusions are made from the study:

1. The uncoated T22 steel indicated severe corrosion. From the XRD analysis of specimens it is found that Fe_2O_3 phase was formed in all three bare boiler steels.
2. The Al_2O_3 -CNT coated T22 boiler steel indicated low weight gain as compared to weight gain by bare and Al_2O_3 coated T22 boiler steel.
3. For T22 steel, the Al_2O_3 -1.5% CNT, Al_2O_3 -2% CNT and Al_2O_3 -4% CNT coatings were successful to reduce the overall weight gain rate by 67.22% , 84.17% and 90.23% of that of bare T22 steel for 10 cycles of the study.
4. The hot corrosion resistance of all the coatings in actual boiler environment can be arranged in the following sequence: Al_2O_3 -4% CNT > Al_2O_3 -2% CNT > Al_2O_3 -1.5% CNT > Al_2O_3
5. The presence of C as shown in elemental analysis indicated the presence and uniform distribution of CNTs in the oxide scale.

6. REFERENCES

- [1] T. Sidhu, S. Prakash, and R. Agrawal, "Hot corrosion and performance of nickel-based coatings," *Current science*, No. 90, 2006.
- [2] H. Singh, D. Puri, and S. Prakash, "High Temperature Oxidation Behaviour of Plasma Sprayed NiCrAlY Coatings on Ni-Based Superalloys in Air," *Trans. Indian Inst. Met.* Vol. 59, pp. 215-227, 2005.
- [3] H. Singh, T. Sidhu, J. Karthikeyan, and S. Kalsi, "Evaluation of characteristics and behavior of cold sprayed Ni-20Cr coating at elevated temperature in waste incinerator plant," *Surface and Coatings Technology*, Vol. 261, pp. 375-384, 2015.
- [4] N. Eliaz, G. Shemesh, and R. Latanision, "Hot corrosion in gas turbine components," *Engineering Failure Analysis*, Vol. 9, No. 1, pp. 31-43, 2002.
- [5] A. López, M. Proy, V. Utrilla, E. Otero, and J. Rams, "High-temperature corrosion behavior of Ni-50Cr coating deposited by high velocity oxygen-fuel technique on low alloy ferritic steel," *Materials & Design*, Vol. 59, pp. 94-102, 2014.
- [6] A. S. Sabau and I. G. Wright, "Influence of oxide growth and metal creep on strain development in the steam-side oxide in boiler tubes," *Oxidation of Metals*, Vol. 73, No. 5-6, pp. 467-492, 2010.
- [7] K. Goyal and R. Goyal, "Performance of Cr 3 C 2-25 (Ni-20Cr) and Ni-20Cr Coatings on T91 Boiler Tube Steel in Simulated Boiler Environment at 900°C," *Chemical and Materials Engineering*, Vol. 4, No. 4, pp. 57-64, 2016.
- [8] X. Zhang, X. Zhang, X. Jie, X. Jie, L. Zhang, L. Zhang, et al., "Improving the high-temperature oxidation resistance of H13 steel by laser cladding with a WC/Co-Cr alloy coating," *Anti-Corrosion Methods and Materials*, Vol. 63, No. 3, pp. 171-176, 2016.
- [9] K. Goyal, H. Singh, and R. Bhatia, "Current Status of Thermal Spray Coatings for High Temperature Corrosion Resistance of Boiler Steel."
- [10] K. Goyal, H. Singh, and R. Bhatia, "Current Status of Thermal Spray Coatings for High Temperature Corrosion Resistance of Boiler Steel," *Journal of Materials & Metallurgical Engineering*, Vol. 6, No. 1, pp. 29-35, 2016.
- [11] L. Erickson, R. Westergård, U. Wiklund, N. Axen, H. Hawthorne, and S. Hogmark, "Cohesion in plasma-sprayed coatings—a comparison between evaluation methods," *Wear*, Vol. 214, No. 1, pp. 30-37, 1998.
- [12] K. Katiki, S. Yadlapati, and S. N. S. Chidepudi, "Comparative High Temperature Corrosion Studies on Zirconium Dioxide Coated Inconel 625 in Air and Molten Salt Environment," *International Journal of ChemTech Research*, Vol. 6, No. 11, pp. 4579-45845, 2014.
- [13] U. Schulz, C. Leyens, K. Fritscher, M. Peters, B. Saruhan-Brings, O. Lavigne, et al., "Some recent trends in research and technology of advanced thermal barrier coatings," *Aerospace science and technology*, Vol. 7, No. 1, pp. 73-80, 2003.
- [14] B. S. Sidhu, D. Puri, and S. Prakash, "Mechanical and metallurgical properties of plasma sprayed and laser remelted Ni-20Cr and Stellite-6 coatings," *Journal of Materials Processing Technology*, Vol. 159, No. 3, pp. 347-355, 2005.
- [15] J. KARTHIKEYAN, K. Sreekumar, N. VENKATRAMANI, and V. Rohatgi, "Preparation and characterization of plasma-sprayed thick ceramic coatings reinforced with metal pins," *High Temperatures. High Pressures*, Vol. 20, No. 6, pp. 653-660, 1988.
- [16] L. Du, W. Zhang, W. Liu, and J. Zhang, "Preparation and characterization of plasma sprayed Ni 3 Al-hBN composite coating," *Surface and Coatings Technology*, Vol. 205, No. 7, pp. 2419-2424, 2010.

- [17] N. Hegazy, M. Shoeib, S. Abdel-Samea, and H. Abdel-Kader, "Effect of plasma sprayed alumina coating on corrosion resistance," in Proc. 13th Int. Conf. on 'Aerospace sciences and aviation technology', Cairo, Egypt, 2009, pp. 1-10.
- [18] E. Celik, I. Ozdemir, E. Avci, and Y. Tsunekawa, "Corrosion behaviour of plasma sprayed coatings," surface and coatings technology, Vol. 193, No. 1, pp. 297-302, 2005.
- [19] S. Deshpande, A. Kulkarni, S. Sampath, and H. Herman, "Application of image analysis for characterization of porosity in thermal spray coatings and correlation with small angle neutron scattering," Surface and coatings technology, Vol. 187, No. 1, pp. 6-16, 2004.
- [20] S. Deshpande, S. Sampath, and H. Zhang, "Mechanisms of oxidation and its role in microstructural evolution of metallic thermal spray coatings—Case study for Ni–Al," Surface and Coatings Technology, Vol. 200, No. 18, pp. 5395-5406, 2006.
- [21] S. Kamal, R. Jayaganthan, and S. Prakash, "Evaluation of cyclic hot corrosion behaviour of detonation gun sprayed Cr 3 C 2–25% NiCr coatings on nickel-and iron-based superalloys," Surface and coatings technology, Vol. 203, No. 8, pp. 1004-1013, 2009.
- [22] M. Hajian Foroushani, M. Shamanian, M. Salehi, and F. Davar, "Porosity analysis and oxidation behavior of plasma sprayed YSZ and YSZ/LaPO4 abradable thermal barrier coatings," Ceramics International, Vol. 42, No. 14, pp. 15868-15875, 11/1/ 2016.
- [23] M. K. Singla, H. Singh, and V. Chawla, "Thermal Sprayed CNT Reinforced Nanocomposite Coatings—A Review," J. Miner. Mater. Charact. Eng, Vol. 10, No. 8, pp. 717-726, 2011.
- [24] Z. Han and A. Fina, "Thermal conductivity of carbon nanotubes and their polymer nanocomposites: a review," Progress in polymer science, Vol. 36, No. 7, pp. 914-944, 2011.
- [25] K. Liew, X. He, and C. Wong, "On the study of elastic and plastic properties of multi-walled carbon nanotubes under axial tension using molecular dynamics simulation," Acta Materialia, Vol. 52, No. 9, pp. 2521-2527, 2004.
- [26] M.-F. Yu, O. Lourie, M. J. Dyer, K. Moloni, T. F. Kelly, and R. S. Ruoff, "Strength and breaking mechanism of multiwalled carbon nanotubes under tensile load," Science, Vol. 287, No. 5453, pp. 637-640, 2000.
- [27] M. Loos, "Chapter 3 - Allotropes of Carbon and Carbon Nanotubes," in Carbon Nanotube Reinforced Composites, M. Loos, Ed., ed Oxford: William Andrew Publishing, 2015, pp. 73-101.
- [28] A. A. Ali, A. Eldesouky, and S. H. Zoalfakar, "Mechanical and tribological properties of hot-pressed electrospun MWCNTs/carbon nanofibril composite fabrics," The International Journal of Advanced Manufacturing Technology, Vol. 74, No. 5-8, pp. 983-993, 2014.
- [29] C. I. Park, M. Mostofa, M. Mahmoodi, and S. S. Park, "Micromechanical scribing and indentation behavior of injection-molded polymeric carbon nanotube (CNT) nanocomposites," The International Journal of Advanced Manufacturing Technology, Vol. 68, No. 1-4, pp. 391-405, 2013.
- [30] A. A. Ali, M. El-Meniawi, and S. Khafagi, "A novel Bi-processing technique for metal matrix nanocomposites," The International Journal of Advanced Manufacturing Technology, Vol. 78, No. 5-8, pp. 907-915, 2015.
- [31] X. Chen, C. Chen, H. Xiao, F. Cheng, G. Zhang, and G. Yi, "Corrosion behavior of carbon nanotubes–Ni composite coating," Surface and Coatings Technology, Vol. 191, No. 2, pp. 351-356, 2005.
- [32] B. Praveen, T. Venkatesha, Y. A. Naik, and K. Prashantha, "Corrosion studies of carbon nanotubes–Zn composite coating," Surface and Coatings Technology, Vol. 201, No. 12, pp. 5836-5842, 2007.
- [33] A. K. Keshri, V. Singh, J. Huang, S. Seal, W. Choi, and A. Agarwal, "Intermediate temperature tribological behavior of carbon nanotube reinforced plasma sprayed aluminum oxide coating," Surface and Coatings Technology, Vol. 204, No. 11, pp. 1847-1855, 2010.
- [34] C. F. Gutierrez-Gonzalez, A. Smirnov, A. Centeno, A. Fernández, B. Alonso, V. G. Rocha, et al., "Wear behavior of graphene/alumina composite," Ceramics International, Vol. 41, No. 6, pp. 7434-7438, 7// 2015.
- [35] M. O. Bodunrin, K. K. Alaneme, and L. H. Chown, "Aluminium matrix hybrid composites: a review of reinforcement philosophies; mechanical, corrosion and tribological characteristics," Journal of Materials Research and Technology, Vol. 4, No. 4, pp. 434-445, 2015.
- [36] W. Guo and H.-Y. Tam, "Effects of carbon nanotubes on wear of WC/Co micropunches," The International Journal of Advanced Manufacturing Technology, Vol. 72, No. 1-4, pp. 269-275, 2014/04/01 2014.
- [37] N. Jegadeeswaran, M. Ramesh, and K. U. Bhat, "Hot Corrosion Studies on As-received and HVOF Sprayed Al 2 O 3+ CoCrAlTaY on Ti-31 Alloy in Salt Environment," Procedia Engineering, Vol. 64, pp. 1013-1019, 2013.
- [38] B. S. Sidhu and S. Prakash, "Studies on the behaviour of stellite-6 as plasma sprayed and laser remelted coatings in molten salt environment at 900 C under cyclic conditions," Journal of materials processing technology, Vol. 172, No. 1, pp. 52-63, 2006.
- [39] B. Singh, A. Jain, and V. Chawla, "Evaluation of erosion-corrosion resistance of some detonation gun sprayed coatings on grade A-1 boiler steel in a coal fired boiler," IOSRD International Journal of Engineering, Vol. 2, No. 1, pp. 13-18, 2015.
- [40] M. Ramesh, S. Prakash, S. Nath, P. K. Sapra, and N. Krishnamurthy, "Evaluation of thermocyclic oxidation behavior of HVOF-sprayed NiCrFeSiB coatings on boiler tube steels," Journal of thermal spray technology, Vol. 20, No. 5, pp. 992-1000, 2011.
- [41] V. Chawla, A. Chawla, D. Puri, S. Prakash, P. G. Gurbuxani, and B. S. Sidhu, "Hot corrosion & erosion problems in coal based power plants in India and possible solutions—a review," Journal of minerals and materials characterization and Engineering, Vol. 10, No. 04, p. 367, 2011.
- [42] V. Chawla, "Microstructural characteristics and mechanical properties of nanostructured and conventional TiAlN and AlCrN coatings on ASTM-SA210 grade A-1 boiler steel," ISRN Corrosion, Vol. 2013, pp. 1-14, 2013.
- [43] B. Somasundaram, R. Kadoli, and M. Ramesh, "Evaluation of Thermocyclic Oxidation Behavior of HVOF Sprayed (Cr 3 C 2-35% NiCr)+ 5% Si Coatings on Boiler Tube Steels," Procedia Materials Science, Vol. 5, pp. 398-407, 2014.
- [44] L. Zhu, S. Zhu, and F. Wang, "Hot corrosion behaviour of a Ni+ CrAlYSiN composite coating in Na 2 SO 4–25wt.% NaCl melt," Applied Surface Science, Vol. 268, pp. 103-110, 2013.
- [45] G. N. Singh and T. Singh, "To Study High Temperature Erosion-Corrosion of Detonation Gun Sprayed Al2O3 Coated and Uncoated T-91 Boiler steel in Actual Environment of Boiler," International Journal of Science and Research, Vol. 3, No. 3, pp. 260-264, 2014.
- [46] N. Bala, H. Singh, and S. Prakash, "High Temperature Corrosion Behavior of Cold Spray Ni-20Cr Coating on Boiler Steel in Molten Salt Environment at 900 C," Journal of thermal spray technology, Vol. 19, No. 1-2, pp. 110-118, 2010.
- [47] D. Gond, V. Chawla, D. Puri, and S. Prakash, "Oxidation Studies of T-91 and T-22 Boiler Steels in Air at 900 C," Journal of Minerals and Materials Characterization and Engineering, Vol. 9, No. 08, p. 749, 2010.
- [48] P. Niranatlumpong, C. Ponton, and H. Evans, "The failure of protective oxides on plasma-sprayed NiCrAlY overlay coatings," Oxidation of Metals, Vol. 53, No. 3-4, pp. 241-258, 2000.
- [49] B. S. Sidhu and S. Prakash, "Erosion-corrosion of plasma as sprayed and laser remelted Stellite-6 coatings in a coal fired boiler," Wear, Vol. 260, No. 9, pp. 1035-1044, 2006.
- [50] V. Chawla, "Structural Characterization and Corrosion Behavior of Nanostructured TiAlN and AlCrN Thin Coatings in 3 wt% NaCl Solution," Journal of Materials Science and Engineering. A, Vol. 3, No. 1A, p. 22, 2013.
- [51] I. Ahmad, M. Unwin, H. Cao, H. Chen, H. Zhao, A. Kennedy, et al., "Multi-walled carbon nanotubes reinforced Al 2 O 3 nanocomposites: mechanical properties and interfacial investigations," Composites Science and Technology, Vol. 70, No. 8, pp. 1199-1206, 2010.